

# Miniaturized and Thermal-Based Measurement System to Measure Moisture in Textile Materials

David Schönfisch, Michael Göddel, Jörg Blinn, Christian Heyde, Heiko Schlarb, Wim Deferme, and Antoni Picard\*

Moisture in textile materials worn close to the skin greatly influences our daily comfort. The measurement of moisture in textile materials is therefore of great interest, for example, to determine the amount of perspiration in clothing or car seats, the wound fluid in dressings, or even the urine in diapers or bed linen. All these applications require a robust moisture measurement method, which is harmless to humans and measures in thin layers. One method ideally suited to fit these requirements is the transient-heat moisture sensing (THMS) method. Herein, a miniaturized and evolved adaption of the THMS method is shown. The measurement system presented herein is optimized for low energy consumption and portability. The working principle of this measuring system is demonstrated by conducting a simple test to investigate the transplanar wicking of eight fundamentally different but garment-typical textiles. The THMS method and its ability to measure in thin layers that is ideally suited to measure moisture in thin layers are shown. Finally, it lays a foundation to enable a multitude of future applications, wherever moisture (e.g., sweat) is to be measured with high accuracy and with a wearable system close to the human skin.

plane source (TPS) method to measure the thermal properties of materials.<sup>[1]</sup> The TPS method is used nowadays in modified forms in many areas, e.g., for the determination of liquid compositions, moisture in skin, or in soils.<sup>[2–4]</sup> The THMS method is specifically adopted in design and data processing to the requirements of moisture measurement in thin textile layers. It is built as a very thin and flat sensor, which has a very favorable ratio of surface to volume. Due to its small volume, the heat capacity ( $[C] = J K^{-1}$ ) is very low and the comparatively large surface ensures a good thermal coupling to the environment (low thermal resistance ( $[R_{TH}] = K W^{-1}$ )). The THMS method differs from other moisture measurement methods. It enables to measure in very thin layers with a low energy effort and with low cross-sensitivity to, e.g., salinity, contact with the human body, or changing ambient temperature.<sup>[5]</sup> Because THMS-based sensors are very slim, inte-


gration on or between thin textile layers is easily possible. In combination with its very moderate energy consumption, the THMS method is therefore predestined to measure moisture in thin textile materials and close to the human body. This could be used, for example, to determine the sweat rate of athletes or characterize different pieces of clothing. To use THMS in garments, it is important to understand how such textiles absorb and bind moisture. The transport of moisture from one side of

## 1. Introduction

Textiles are used for many different purposes and we come into daily contact with them. Moisture measurements in textiles can be conducted for a variety of reasons, such as to determine the amount of perspiration in clothing, wound fluid in bandages, or even urine in diapers or bed linen. The transient-heat moisture sensing (THMS) method is a principle similar to the transient

D. Schönfisch, M. Göddel, J. Blinn, Prof. A. Picard  
Department of Informatics and Micro Systems Technology  
University of Applied Sciences Kaiserslautern  
Amerikastraße 1, Zweibrücken 66482, Germany  
E-mail: Antoni.Picard@hs-kl.de

Dr. C. Heyde  
Future Sport Science  
Adidas AG  
Herzogenaurach 91074, Bavaria, Germany

 The ORCID identification number(s) for the author(s) of this article can be found under <https://doi.org/10.1002/pssa.201900835>.

© 2020 The Authors. Published by WILEY-VCH Verlag GmbH & Co. KGaA, Weinheim. This is an open access article under the terms of the Creative Commons Attribution-NonCommercial License, which permits use, distribution and reproduction in any medium, provided the original work is properly cited and is not used for commercial purposes.

DOI: 10.1002/pssa.201900835

H. Schlarb  
Advanced Creation – Testing  
Adidas AG  
Herzogenaurach 91074, Bavaria, Germany

Prof. W. Deferme  
Institute for Materials Research (IMO)  
Hasselt University  
Diepenbeek 3590, Belgium

Prof. W. Deferme  
Division IMOMEC  
IMEC VZW  
Wetenschapspark 1, Diepenbeek 3590, Belgium

the textile to the other is usually called “transplanar wicking.” Some textiles, which are used, e.g., for sportswear, are designed to actively transport moisture from their inside to their outside.<sup>[6]</sup> This increases the wearing comfort and improves the evaporation on the textile surface. There are no official standards for the investigation of transplanar wicking, but there are various methods available.<sup>[7]</sup> Many of these methods determine how much water a textile absorbs under given circumstances and how much it evaporates on the surface. Only few of these methods are able to determine where the moisture is bound in the textile.<sup>[8]</sup> However, these mostly use an electrically resistive method to indicate the moisture content. Thus, it is necessary to use a standardized perspiration solution with known conductivity. In addition, it is not possible to use it during evaporation, as this also influences the ion concentration and therefore the conductivity of the liquid.

This work shows how it is possible to investigate the transplanar wicking of textiles with the THMS method. Furthermore, it lays a foundation for later portable applications.

## 2. Theoretical Basics

### 2.1. THMS

We already presented and explained the THMS method in detail in an earlier study.<sup>[5]</sup> It uses the changing thermal properties of porous materials when they absorb water.<sup>[9]</sup> This can be attributed to the different volumetric specific heat capacity ( $c_v$ ) and thermal conductivity ( $\lambda$ ) of water ( $c_v = 4.2 \times 10^6 \text{ J m}^{-3} \text{ K}^{-1}$ ;  $\lambda = 0.60 \text{ W m}^{-1} \text{ K}^{-1}$ ) compared with air ( $c_v = 1.2 \times 10^3 \text{ J m}^{-3} \text{ K}^{-1}$ ;  $\lambda = 0.026 \text{ W m}^{-1} \text{ K}^{-1}$ ). The human perception of moisture is also strongly determined by thermal perception. Thus, the contact temperature during the touching of moist materials is an important factor for the perception of moisture via the skin.<sup>[10,11]</sup> The contact temperature of two homogeneous materials, assumed to be semi-infinite, is only determined by their temperatures and thermal effusivities (valid for nonstationary cases).<sup>[12]</sup> The thermal effusivity ( $e$ ) of a material (sometimes referred to as thermal penetration coefficient or thermal inertia) is composed of its thermal conductivity and volumetric heat capacity

$$e = \sqrt{\lambda \cdot c_v} \quad (1)$$

The THMS sensor consists of a thin resistor that is briefly heated by joule heating. During this heating, the temperature of the THMS increases and at the same time heat is dissipated through the immediate environment (e.g., the textile). This heat dissipation depends on the thermal properties of the environment. In the end, the sensor heats up more in a dry environment than in a moistened one. Due to the positive temperature coefficient resistor behavior of the THMS sensor element, the relative resistance increase ( $\Delta R R_0^{-1}$ ) is proportionally linked to the temperature increase ( $\Delta\theta$ ). This relationship is defined by the temperature coefficient of the electrical resistance ( $\alpha_{\text{TCR}}$ ) of the sensor

$$\frac{\Delta R}{R_0} = \Delta\theta \cdot \alpha_{\text{TCR}} \quad (2)$$

Under certain simplifications, the temperature rise of the sensor with transient heating can be assumed to be

approximately linearly dependent on the root of the heating time.<sup>[13,14]</sup> Ultimately, it can be described as a function of time ( $t$ ), of heating power per area ( $[q] = \text{J s}^{-1} \text{ m}^{-2}$ ), and of the thermal effusivity ( $e$ ) of the environment<sup>[15]</sup>

$$\Delta\theta(t) = \frac{2q}{e\sqrt{\pi}} \sqrt{t} \quad (3)$$

The THMS sensor should measure the moisture content of the material in the immediate environment. However, the further environment should not influence the sensor signal. This is possible because the heat is transferred through the touching environment (textile) with only a limited rate. After the start of transient heating, the heat spreads like diffusion from the sensor over the surrounding textile into the further environment. This spreading of temperature ( $\delta_{\text{pd}}$ ) is a function of the thermal diffusivity ( $\alpha = \lambda/c_p$ ) of the ambient and the heating time ( $t_p$ ).  $\delta_{\text{pd}}$  is often referred to as effective thermal diffusion length<sup>[15,16]</sup>

$$\delta_{\text{pd}} \sim \sqrt{\alpha \cdot t_p} \quad (4)$$

By appropriate temporal discrimination, the influence of the further environment can be demarcated. The sensor signal ( $S$ ) is defined according to the thermal effusivity ( $e$ ) and in a certain time frame ( $\Delta$  from  $t_{\text{min}}$  to  $t_{\text{max}}$ )

$$S \sim e \sim \frac{\Delta \sqrt{t}}{\Delta\theta(t)} \quad (5)$$

### 2.2. Textile Liquid Moisture Management

There are many different mechanisms influencing the liquid moisture transport in fabrics. It can be roughly separated into wetting of the fabric surface and wicking through it. The main mechanism of the moisture transport through a textile is due to capillary action, whereas, e.g., diffusion plays a subordinate role due to its very slow nature. The probably simplest case of capillary wicking is the one in a single tube with a circular cross-section. The pressure ( $\Delta P$ ) with which water is wicked into a capillary can be described by Young–Laplace’s equation<sup>[17]</sup>

$$\Delta P = \frac{2\gamma \cos(\theta)}{R} \quad (6)$$

This is greatly simplified, and the description of complete textiles with many differently shaped pores is considerably more complex. Nevertheless, this simple formula shows three main quantities that are responsible for moisture transport—the radius ( $R$ ) of the capillary, the surface tension ( $\gamma$ ) of the liquid-to-air interface, and the contact angle of liquid to fiber material ( $\theta$ ). Although, the surface tension is given by the liquid, capillary radius and contact angle can be modified for textiles, e.g., by fiber/yarn density and by fiber material or surface modification of them.

## 3. Methods

### 3.1. THMS Sensor

The THMS sensor itself is a nickel conductor with a thickness of  $\approx 900 \text{ nm}$  embedded between two isolating layers of

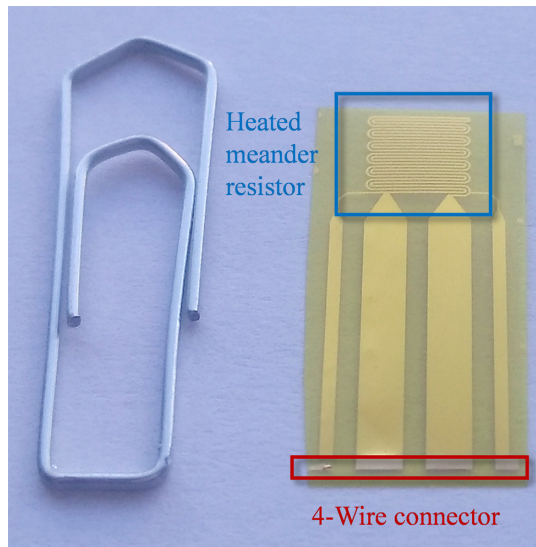


**Figure 1.** Sensor manufactured with microfabrication technologies. Nickel meander resistor (as shown in the blue rectangle) embedded and electrically isolated between two layers of polyimide. The upper cover layer is open at four-wire contact pads at the bottom (red rectangle) to be soldered to wires or a printed circuit board.

≈10 μm-thick polyimide (as shown in **Figure 1**). The TCR of the nickel thin film was determined experimentally with  $\alpha_{\text{TCR}}$  of about  $(6.5 \pm 0.10) \times 10^{-3} \text{ K}^{-1}$  (measured in a temperature range from 20 to 110 °C; see Supporting Information). The fabricated thin-film heaters have an average resistance of about  $114 \pm 3.6 \Omega$  (at room temperature of ≈21 °C, mean value, and sample standard deviation of 14 sensors) and a rectangular shape of  $5 \times 5 \text{ mm}^2$ . The line width and the spacing of the meander lines are about ≈100 μm. There are also four contact pads on the polyimide film to solder the sensors and allow optional use of four-terminal sensing technology. The process flow for the fabrication of the sensor elements can be found in Supporting Information.

### 3.2. Measurement Electronics

**Figure 2** shows the measuring system with two THMS sensors. The contact pads of the THMS nickel heater are soldered to a small printed circuit board (PCB).

Each of these sensor PCBs has its own analog-to-digital converter (ADC, ADS1115, with 16 bit) and a Wheatstone bridge. Up to eight sensors can be connected to the central control unit with a microcontroller (FireBeetle ESP32), an interintegrated circuit (I<sup>2</sup>C) switch (TCA9548A, with eight channels), and further electronics for the generation of short voltage pulses. Only five channels are used for the following measurements. A schematic illustration of the measurement system circuit is shown in **Figure 3**. The resistors ( $R_1$  and  $R_3$ ) and the trimmer resistor ( $R_2$ ) at the cold arm of the Wheatstone bridge have a high resistance (≈2 kΩ each, to keep energy consumption and self-heating low), whereas the sensor ( $R_{\text{Sens}}$ ) and its series resistor ( $R_4$ ) have a lower resistance (≈100 Ω).  $R_4$  has a high thermal capacity and, like the other resistors  $R_1$ ,  $R_2$ , and  $R_3$ , also a low TCR and a good

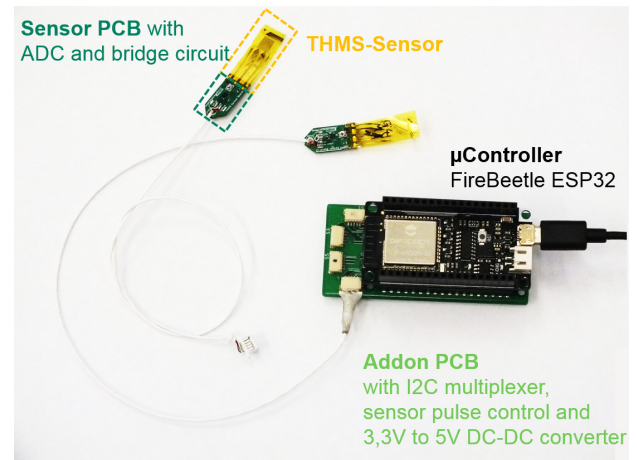


**Figure 2.** Measurement system with two THMS sensors. Up to eight sensors can be connected to the central control unit (Addon PCB with ESP32 Development Board) and used simultaneously.

thermal coupling to the ambient (sensor PCB). This prevents the resistors from changing their resistance during the heating of the sensor ( $R_{\text{Sens}}$ ). The placement of the ADC close to the sensor allows precise measurement of resistance changes without electric interferences due to longer cables.

The bridge voltage measurement data points of the sensor PCBs are transferred via an I<sup>2</sup>C (a serial computer bus) to a central control unit. This unit generates voltage pulses (of  $U_{\text{Supply}} = 5 \text{ V}$ ) to heat the sensors and simultaneously controls the ADCs, which measure bridge voltage. The variable sampling rate of the ADC is set to 128 samples per second (SPS), i.e., the interval between the measuring points is about 7.9 ms. One voltage pulse lasts about ≈300 ms. The sample rate is a good compromise between the precise determination of the slope (many data points) and easy calculation of the slope with the microcontroller (few data points). The very short pulse length and the low voltage result in an energy consumption below 40 mJ per measurement to heat the sensor and resistance network. For a sampling rate of one acquisition per minute (e.g., to track sweating), this results in less than 0.7 mW average power. This would be low enough to run the circuit on a typical wearable battery for several days (energy consumption of the central control unit not included).

The microcontroller collects the bridge voltage samples in the time range from ≈50 to ≈300 ms (≈ 34 samples) to calculate the sensor signal ( $S$ ) with a simple linear regression algorithm according to

$$S = \frac{\sum_i^n (U_{B_i} - U_{B_m})(\sqrt{t_i} - \sqrt{t_m})}{\sum_i (U_{B_i} - U_{B_m})^2} \quad (7)$$

where  $U_{B_m}$  and  $t_m$  are the mean values of the bridge voltage samples ( $U_{B_i}$ ) and time points ( $t_i$ ). The time range was chosen to measure in textile layers with a thickness below ≈0.4 mm and to gain a linear dependency between the measured bridge voltage and the square root of the heating time. The impact of moisture or other environmental influences from a distance more than ≈0.4 mm is negligible due to the limitation of the heat pulse

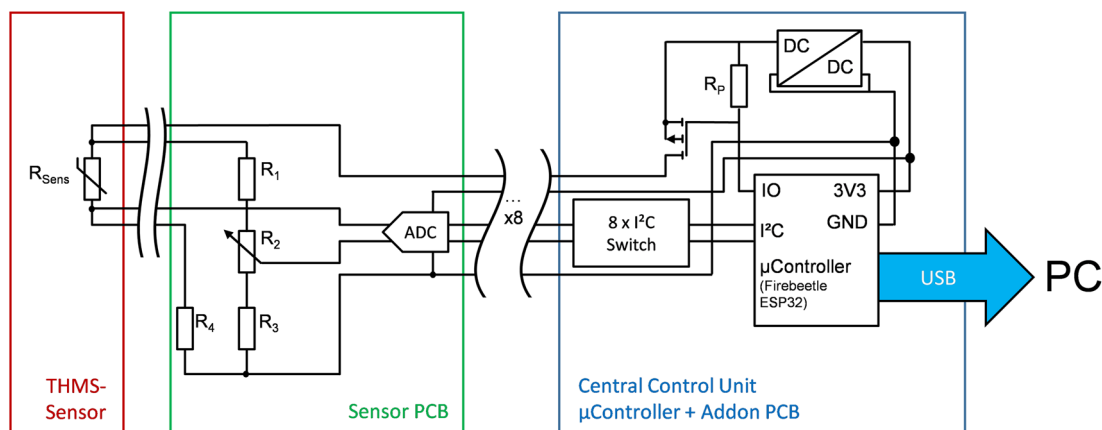


**Figure 3.** Schematic illustration of the measurement system. Up to eight sensors (sensor PCB and THMS sensor) can be connected to the central control unit and used simultaneously.

and measuring time period (according to Equation (4)): the longer the time, the further it reaches the sensitive area. The full-scale output of the sensor signal can be determined by operating the sensors once in free air and once dipped completely in water. This also enables the comparison of the sensitivity and homogeneity of several fabricated sensors.

The temperature increase due to the heat pulse can be approximated with Equation (2) and the bridge voltage increase according to

$$\Delta\vartheta = \frac{\Delta R}{R_0} \cdot \frac{1}{\alpha_{\text{TCR}}} \approx \frac{U_B}{U_{\text{Supply}}} \cdot \frac{4}{\alpha_{\text{TCR}}} \quad (8)$$

### 3.3. Plate Measurement Setup and Fabric Selection

To be able to test the measuring system with several different textiles, we glued five sensors on a support plate with a double-sided adhesive tape (Tesa SE – tesafix 4965;  $\approx 205 \mu\text{m}$  thick). The plate and the tape have a low thermal conductivity and heat capacity. The textiles under test are placed on top of the sensor arrangement. The combined thermal effusivity ( $e_{\text{comb}}$ ) of the plate and textile can be estimated analogously to the electrical parallel connection of two admittances<sup>[18]</sup>

$$e_{\text{comb}} = \frac{e_{\text{Textile}} + e_{\text{Plate}}}{2} \quad (9)$$

The measuring signal is therefore reduced compared with an arrangement with double-sided textile layers.

The sensor plate setup with five mounted sensors is shown in **Figure 4a**. All textile samples have a size of about  $12.5 \text{ cm} \times 12.5 \text{ cm}$ . **Table 1** shows an overview of the eight different textiles used in this work.

To estimate the full-scale output of the sensor signal and the effect of gluing on the supporting plate, the sensor signal was determined in a previous test for air and 100% water. For the water measurement, a layer of water was applied on top of the plate.

During a measurement, a plate (without sensors) is placed on top of the textile sample to prevent evaporation and establish a

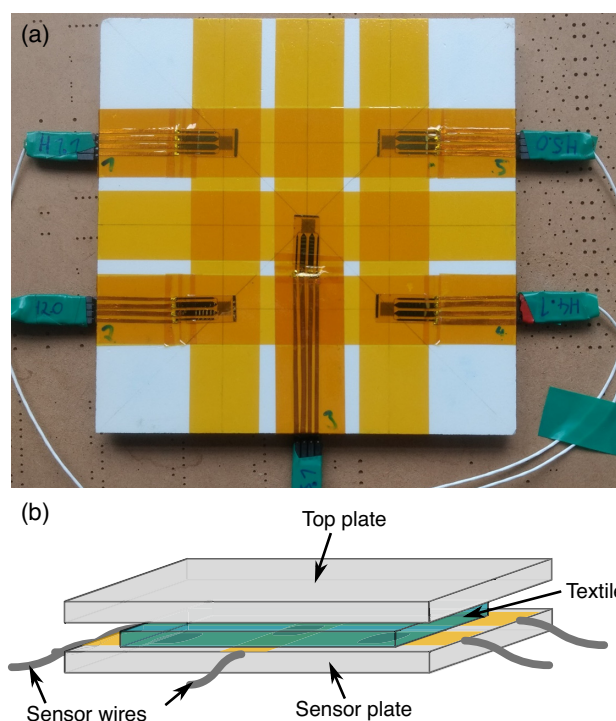


**Figure 4.** a) Photo of the sensor plate with five THMS sensors glued on top. b) Schematic side view of the stack with the sensor plate, textile sample, and top plate for stabilization.

homogenous contact between sensors and the textile. The whole setup is shown schematically in **Figure 4b**. To set different degrees of moisture saturation, we have moistened the textiles with a spray atomizer. During this procedure, the textile hung vertically on a mounting plate (shown in **Figure 5**) and the spray atomizer was at a distance of about  $\approx 30 \text{ cm}$ .

For each moisture level, we applied about ten pump strokes of water ( $\leq 1 \text{ g}$  of water on the textile surface) to the inner face of the textile. The inner face is defined here as the side of the textile, which usually comes in contact with the skin. Only for textiles

**Table 1.** Properties of the different textiles.

Textile code #	Composition	Textile manufacturing technique	Thickness <sup>a)</sup> [mm]	Weight [g m <sup>-2</sup> ]	Bulk density [g cm <sup>-3</sup> ]	Porosity <sup>b)</sup> [%]	Max. absorption capacity per area <sup>c)</sup> [mL m <sup>-2</sup> ]
Fb1	100% cotton	Single jersey	0.53	161	0.30	80	494
Fb2	80% nylon/20% elastane	Warp knit tricot (double)	0.66	230	0.35	70	387
Fb3	100% polyester	Interlock (1 × 1 both sides) (double)	1.18	296	0.25	82	838
Fb4	95% polyester/5% elastane	Spacer knit-3 layers (triple)	0.96	266	0.28	80	870
Fb5	60% polyester/40% polypropylene	Double jersey	0.68	159	0.23	79	556
Fb6	100% polyester	Single jersey	0.46	127	0.28	80	390
Fb7	100% cotton	Woven	0.6	120	0.20	87	435
Fb8	50% polyester/50% polyamide	Nonwoven (microfiber)	0.65	135	0.21	83	574

<sup>a)</sup> Measured at a compression of  $\approx 1 \text{ kg dm}^{-2}$ ; <sup>b)</sup> Calculated according to Hsieh<sup>[19]</sup>; <sup>c)</sup> Maximum amount of water the textile can hold while hanging upright. Based on the LAC measurement method.<sup>[20]</sup>

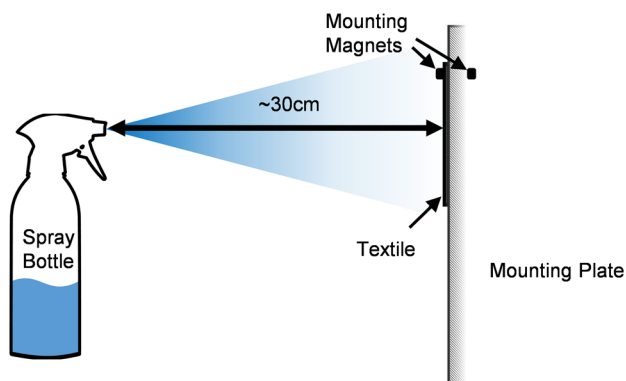


**Figure 5.** Schematic of the procedure to increase the moisture state of the textile.

Fb3 and Fb4, we increased the pump strokes to 20 strokes, due to their very high absorption capacity per area. Except for the textile Fb7, all textiles are typical for garments. Fb7 is a nonwoven textile similar to wiping cloth.

To determine the degree of saturation of the textile, the textiles were weighed before each moisture measurement. The degree of saturation ( $\zeta$ ) is defined here as the actual mass of water inside the textile ( $m_W$ ) in relation to its maximum absorption capacity ( $m_{W_{\max}}$ ) according to

$$\zeta = \frac{m_W}{m_{W_{\max}}} = \frac{m_{\text{WetTextile}} - m_{\text{DryTextile}}}{m_{\text{maxWetTextile}} - m_{\text{maxDryTextile}}} \quad (10)$$

The maximum absorption capacity is measured according to the liquid absorption capacity (LAC) measurement method.<sup>[20]</sup>

Directly after each weighing, the textile is placed on top of the sensor plate with its inner face in the direction of the sensors. After 1 min of measurement, which allows  $\approx 6$  independent moisture measurements, the textile is turned around and the outer face is measured for 1 min.

With the exception of the fabric Fb8, all textiles are typical for clothing, but they all have very different properties. On the

one hand, they differ in fiber material and, on the other hand, they are constructed by different textile manufacturing techniques. Probably one of the most common manufacturing techniques for clothing typical fabrics is the “Single Jersey” knit type. This type is used for Fb1 and Fb6. However, they differ in fiber material. Fb1 is made of cotton, whereas Fb6 is made of polyester. Natural fibers tend to absorb more moisture in their fiber core than synthetic fibers.<sup>[21]</sup> Fabric Fb3 and Fb4 have a very high thickness compared with the other fabrics and, therefore, also a higher liquid absorption capacity. The fabric Fb5 is constructed by two different yarns and has at its inner-face larger pores (i.e., larger interyarn capillaries). Unlike the others, textiles Fb7 and Fb8 are not knitted but woven (Fb7) and felted (Fb8). Furthermore, Fb8 is made of microfibers.

## 4. Measurement Results and Discussion

### 4.1. Sensor Signal Definition

During  $\approx 300 \text{ ms}$  of heating, the core sensor temperature and therefore also the bridge voltage increase. This increase of one THMS sensor once in water and once in air is shown in **Figure 6**. For this test, the sensor was not yet glued to the plate to determine the deviation between the sensors and their maximal heat-up. A temperature increase in maximal 15 K for a time below 1 s can be considered to be harmless and also hard to perceive for humans.<sup>[12]</sup> The bridge voltage and therefore also the temperature increase in the range between  $\approx 50$  and  $\approx 300 \text{ ms}$  are quite linear with the square root of the heating time and are therefore used to calculate the sensor signal. The sensor signal for the measurement in **Figure 6** is calculated accordingly to Equation (7):  $182 \pm 1.2 \text{ s}^{0.5} \text{ V}^{-1}$  for water and  $3.95 \pm 0.03 \text{ s}^{0.5} \text{ V}^{-1}$  for air.

The influences of varying ambient temperature on the sensor signal  $S$  (in  $\text{s}^{0.5} \text{ V}^{-1}$ ) are below  $\approx 0.45 \text{ s}^{0.5} \text{ V}^{-1} \text{ K}^{-1}$  (in the range from 15 to 35 °C). Detailed information on determination can be found in Supporting Information.

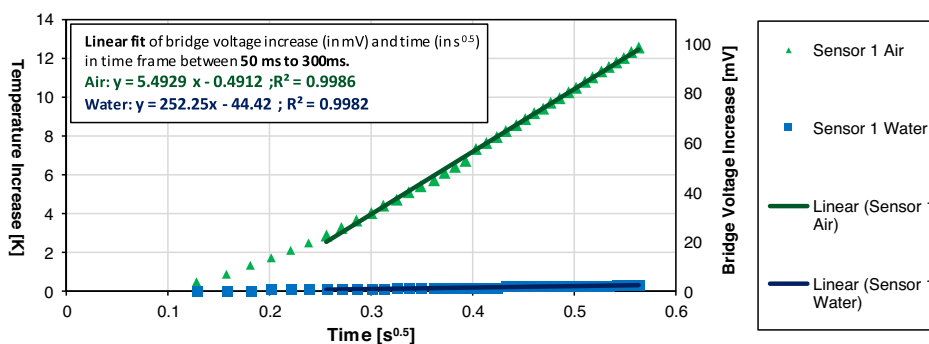


Figure 6. Bridge voltage and assumed sensor core temperature of one THMS sensor if immersed in water or in air.

#### 4.2. Measurement with Plate Setup

Figure 7 shows the mean value and deviation of the five sensors and for 30 measurements in air and water. For the measurements in water, the whole plate with the five sensors was covered with a layer of water. The measured sensor signals of all five sensors were nearly the same. If compared with the results in Figure 6, these values for the sensor signal are damped (lower for water and higher for air) due to the one-sided gluing of the sensors to the plate (as shown in Figure 4a).

An example of the temporal course of the measurement with Fb4 is shown in Figure 8. Each side of the textile was measured for at least 1 min. To measure the second (outer) side, the textile was turned over. After the measurement of both textile sides, the textile was removed from the plate, moistened with the atomizer, and placed back on top of the sensor plate. The results show that there is a low deviation for sequential measurements with the same sensor and same saturation but a larger deviation between the five sensors. This could be due to an inhomogeneous distribution of water across the textile or varying contact between sensors and the textile. The sensors themselves measure very similarly in air and water, as shown in Figure 7.

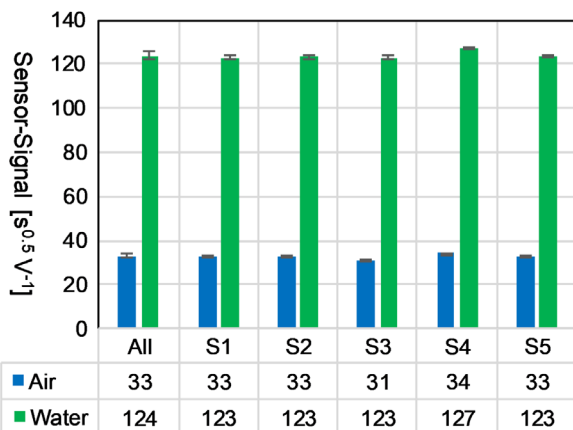


Figure 7. Sensor signal of the five sensors mounted on the sensor plate. Mean value of each of the 30 measurements in air and in water.

#### 4.3. Results of Textile Characterization

The measured sensor signals for the eight different textiles and moisture saturations are shown in Figure 9. The mean value of each of the five sensors and the sample standard deviation between them are shown as one point with corresponding error bars. The mean sensor signals are plotted above the moisture saturation, which is calculated with the textile weight and maximal absorption capacity according to Equation (10). It should be noted that the indicated saturation means the total saturation of the whole fabric. Local differences within the structure are not considered in this value.

Four different moisture management behaviors can be distinguished for the eight textiles and are shown in Figure 10. It should be noted here that this is only a very rough classification. In reality, there are many different properties, which describe the overall moisture management of a textile. The difference between the four types of moisture managements is as follows.

*Type 1:* Homogeneous distribution of moisture in the textile (Fb6, Fb7, and Fb8). The moisture is quickly transported through the textile and evenly distributed. With these textiles, the sensor signal is almost linearly dependent on the saturation state.

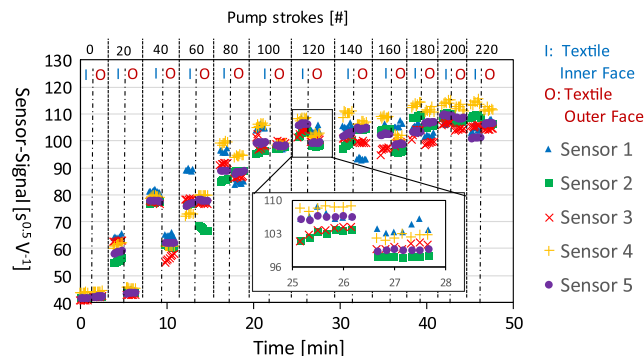
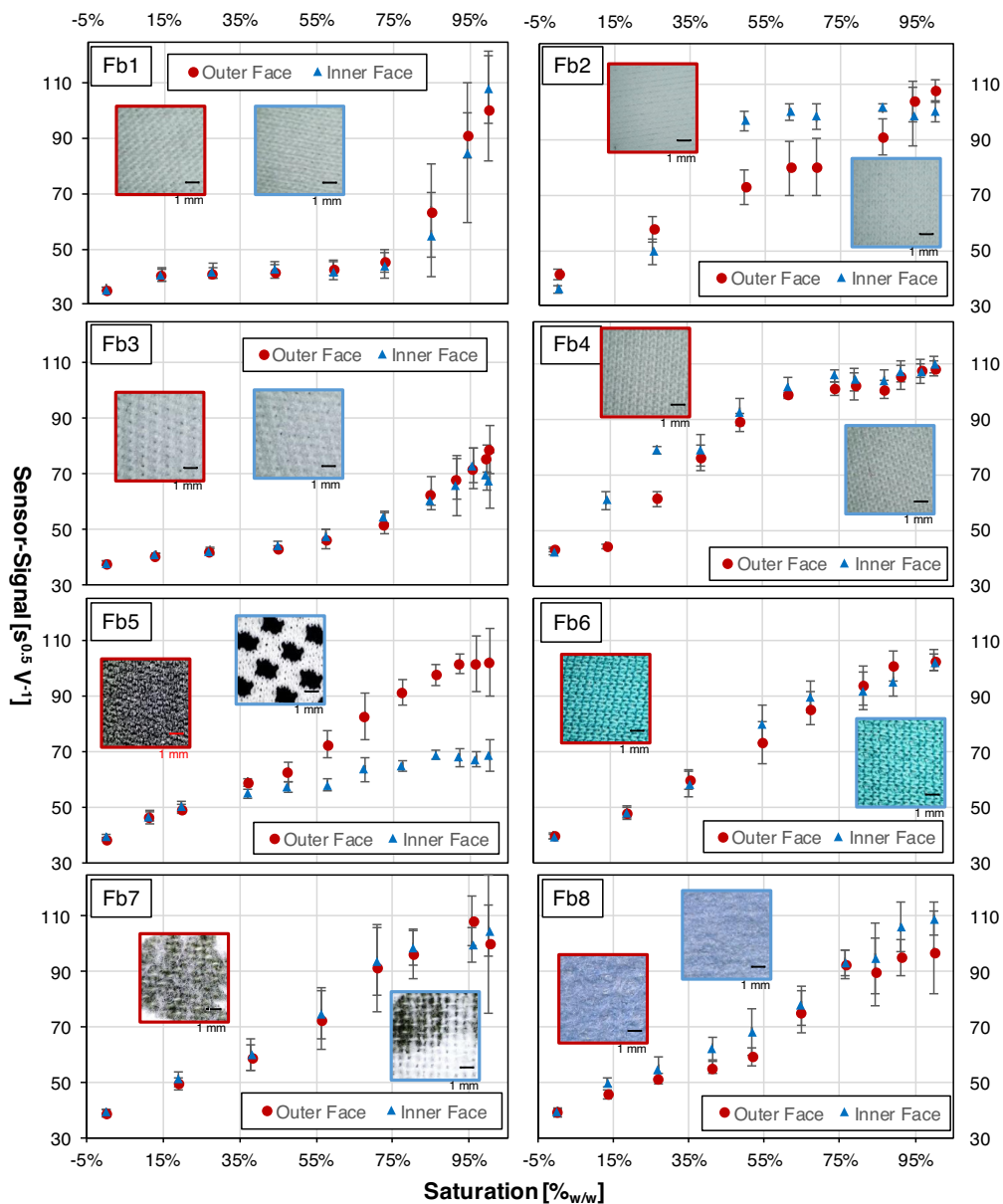


Figure 8. Measurement example with textile Fb4. The moisture saturation of the textile was increased with a water atomizer after each side was measured for 1 min. After each moistening, first the inner side (wetted side) and then the outer side were measured. The five sensors on the measuring plate are each marked in different colors.



**Figure 9.** Sensor signal for the eight different textiles as a function of the textile saturation state. Each point shows the mean value of the five sensors and the error bar shows the sample standard deviation between them.

*Type 2:* Moisture binding in the textile core (Fb1 and Fb3). The moisture is quickly transported away from the inner surface and is stored in the textile core. These textiles show only a slight increase in the sensor signal within the lower saturation range  $<75\%$ . One reason for this behavior could be the increased roughness of the textile surfaces. This also means larger pores between the fibers and the yarn.

*Type 3:* Moisture at textile surfaces (Fb2 and Fb4). The moisture is mainly located on the textile surfaces, whereas water content at the textile core seems to be low. The sensor signal increases steeply directly at the beginning (saturation below  $\approx 25\%$ ). Textile Fb4 is a spacer fabric with two outer textile layers connected by a spacer thread. It has, therefore, very small

pores on the outer surfaces and large ones in the middle. This could result in a capillary suction effect from the textile core to the faces and provoke this moisture management behavior. Furthermore, the sensor signal for the inner surface is slightly higher than that for the outer (Fb2). This could also indicate a very low moisture transport within the textile (e.g., due to the textile thickness).

*Type 4:* Moisture binding on the textile outer surface (Fb5). The sensor signal for the outer surface increases faster than for the inner surface. In this case, the moisture is quickly transported through the textile. Furthermore, it is bound with higher affinity to the textile's outer face than to the inner face (e.g., due to smaller capillaries). Textile Fb5 has a very rough but also

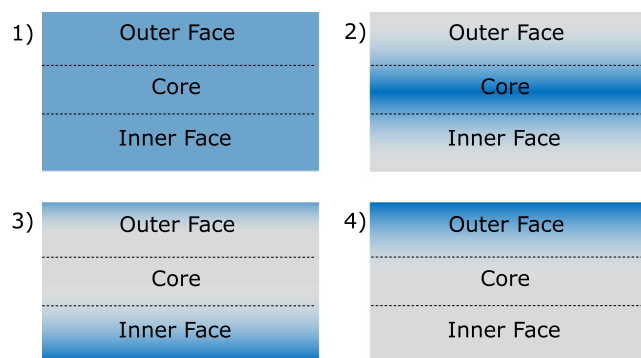


**Figure 10.** Illustration of the four different moisture-management types found for the used textiles.

soft inner face with a low fiber density and large pores (those can be also seen in the photo of the inner face), whereas its outer face is more uniform with a higher fiber density and small pores. A higher fiber density at the outer face in contrast to the inner face of textiles is used to increase moisture wicking and transport to the outer face and also increase the comfort of apparel.<sup>[6]</sup>

## 5. Conclusions

In this work, a miniaturized and evolved moisture measurement system based on the THMS is shown. The basics of this measuring method are discussed and explained in detail. The enhanced THMS method is optimized for low energy consumption and portability. Eight different textiles were characterized to demonstrate the specific capabilities of the THMS system. These textiles have very different properties in structure and fiber material but are typical for clothes. This work shows that the THMS measuring system with its ability to measure in thin layers is ideally suited to investigate the transplanar wicking inside these textiles. The moisture transport properties of the eight textiles could be classified into four types. For example, the textile of type 4 showed an active transport of moisture from the wetted inner face to its outer face. This means that moisture was preferably bound to the outer side. This can be a very advantageous behavior for underwear and sportswear. One can see that the investigation of different textile properties with the THMS method provides basic knowledge for later wearable applications. Therefore, the characterization of textiles and clothing is a promising field of application for THMS. It has considerable advantages over currently established methods, which are mostly based on resistive measurements and prone to cross sensitivity.<sup>[8,22]</sup>

A further example of application for basic physiological research could be derived from the measured properties of type 1 textiles. Type 1 provides a homogeneous moisture distribution over the textile. This behavior could be desirable for later applications in a sweat rate monitor.<sup>[23–25]</sup> With such a measuring system, extended by wireless data transmission, the sweating behavior of athletes could be investigated, e.g., to analyze at which point in time and under which physical stress they start or stop sweating or how the sweat rate distribution develops over

time at all. The advantage of our measuring method lies here in the robust functionality, which is not influenced by contact to the human body, as, e.g., with electrically capacitive or by the salt content, as, e.g., with electrically resistive.

## Supporting Information

Supporting Information is available from the Wiley Online Library or from the author.

## Acknowledgements

This work was financially supported by the Adidas AG and was performed in terms of cooperative doctorate graduation supported by the project “Meeting Point Functional Layers” (MPFL) at the University of Applied Sciences Kaiserslautern. The MPFL is part of the DAAD supporting program of “Strategic Partnerships and Thematic Networks” (project no. 57172293).

## Conflict of Interest

The authors declare no conflict of interest.

## Keywords

moisture sensors, textile moisture, thermal moisture measurements, transient-heat moisture sensing, water contents

Received: October 1, 2019

Revised: March 3, 2020

Published online: April 22, 2020

- [1] S. Gustafsson, *US Patent US5044767A*, **1991**.
- [2] B. Schmitt, A. Schütze, *Sens. Actuators A* **2015**, *235*, 210.
- [3] S. R. Krishnan, C. J. Su, Z. Xie, M. Patel, S. R. Madhupathy, Y. Xu, J. Freudman, B. Ng, S. Y. Heo, H. Wang, T. R. Ray, J. Leshock, I. Stankiewicz, X. Feng, Y. Huang, P. Gutruf, J. A. Rogers, *Small* **2018**, *14*, 1803192.
- [4] D. Fidirková, V. Vretenár, I. Šimková, V. Greif, J. Vlčko, P. Dieška, L. Kubičár, *Int. J. Thermophys.* **2013**, *34*, 1918.
- [5] D. Schönfisch, M. Göddel, J. Blinn, C. Heyde, H. Schlarb, W. Deferme, A. Picard, *Phys. Status Solidi A* **2019**, *216*, 1800765.
- [6] J. Mecheels, *Körper-Klima-Kleidung: Wie Funktioniert Unsere Kleidung?*, Schiele & Schön, Berlin **1998**.
- [7] B. Das, A. Das, V. K. Kothari, R. Fanguiero, M. de Araújo, *Autex Res. J.* **2007**, *7*, 100.
- [8] J. Hu, Y. Li, K.-W. Yeung, A. S. W. Wong, W. Xu, *Text. Res. J.* **2005**, *75*, 57.
- [9] S. Lu, Z. Ju, T. Ren, R. Horton, *Agric. For. Meteorol.* **2009**, *149*, 1693.
- [10] M. Shibahara, K. Sato, *IEEE Trans. Haptics* **2019**, *12*, 533.
- [11] M. Raccuglia, S. Hodder, G. Havenith, *Text. Res. J.* **2016**, *87*, 2449.
- [12] K. C. Parsons, *Human Thermal Environments: The Effects of Hot, Moderate, and Cold Environments on Human Health, Comfort, and Performance*, 3rd ed., CRC Press, Boca Raton, FL **2014**, p. 421, 423.
- [13] S. E. Gustafsson, *Rev. Sci. Instrum.* **1991**, *62*, 797.
- [14] H. S. Carslaw, J. C. Jaeger, *Conduction of Heat in Solids*, Clarendon Press, Oxford **1959**.
- [15] E. Marin, *Lat. Am. J. Phys. Educ.* **2010**, *4*, 56.
- [16] S. E. Gustafsson, E. Karawacki, M. N. Khan, *J. Phys. D: Appl. Phys.* **1979**, *12*, 1411.
- [17] N. Pan, Z. Sun, *Thermal and Moisture Transport in Fibrous Materials*, Elsevier Science, Oxford **2006**.



- [18] S. Jayachandran, R. N. Prithiviraajan, K. S. Reddy, in *AIP Conf. Proc.*, AIP Publishing LLC **2017**, Vol. 1859, p. 020008.
- [19] Y. Hsieh, *Text. Res. J.* **1995**, 65, 299.
- [20] International Organization for Standardization, *Textiles – Test Methods for Nonwovens – Part 6: Absorption (EN/ISO Standard No. 9073-6)* **2003**.
- [21] J. Christie, I. G. Platt, in *2014 IEEE Sensors Applications Symp., SAS 2014, Proc.*, IEEE, Piscataway, NJ, USA **2014**, p. 161.
- [22] P. Kubiak, J. Leśnikowski, K. Gniotek, *Fibres Text. East. Eur.* **2016**, 24, 151.
- [23] H. Ueda, Y. Inoue, *Ergonomics* **2013**, 3, 1000121.
- [24] A. Brueck, T. Iftekhar, A. Stannard, K. Yelamarthi, T. Kaya, *Sensors* **2018**, 18, 533.
- [25] C. J. Smith, G. Havenith, *Eur. J. Appl. Physiol.* **2011**, 111, 1391.